

## **Supplemental Information**

### **Photoactivated Spatiotemporally-Responsive Nanosensors of *In Vivo* Protease Activity**

Jaideep S. Dudani<sup>1,2</sup>, Piyush K. Jain<sup>1,3</sup>, Gabriel A. Kwong<sup>1,3,&</sup>, Kelly R. Stevens<sup>1,3</sup>,  
Sangeeta N. Bhatia<sup>1,3-7,\*</sup>

1. Koch Institute for Integrative Cancer Research, Massachusetts Institute of Technology, Cambridge, MA 02139
2. Department of Biological Engineering, Massachusetts Institute of Technology, Cambridge, MA 02139
3. Institute for Medical Engineering and Science, Massachusetts Institute of Technology, Cambridge, MA 02139
4. Electrical Engineering and Computer Science, Massachusetts Institute of Technology, Cambridge, MA 02139
5. Department of Medicine, Brigham and Women's Hospital and Harvard Medical School, Boston, MA 02115
6. Broad Institute of Massachusetts Institute of Technology and Harvard, Cambridge, MA 02139
7. Howard Hughes Medical Institute, Cambridge, MA 02139
- & Present Address: Wallace H. Coulter Department of Biomedical Engineering, Georgia Tech and Emory School of Medicine, Atlanta, GA 30332

\*Corresponding Author:

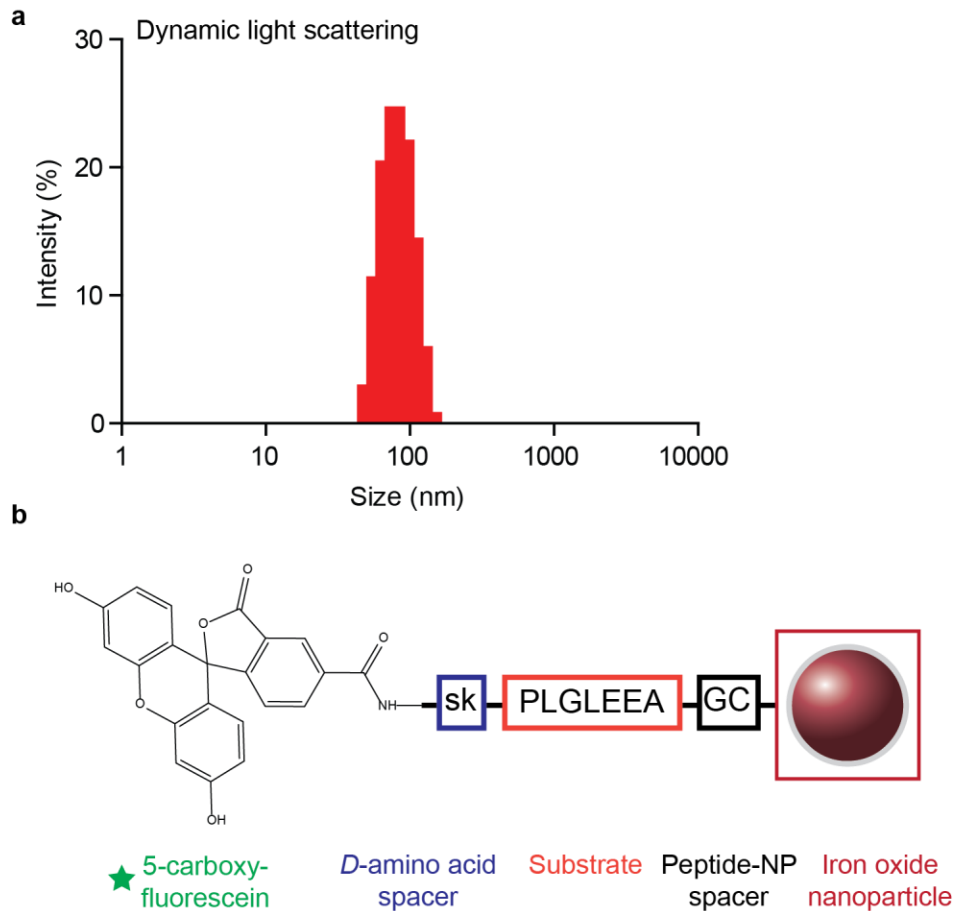
Sangeeta N. Bhatia

Address: 500 Main Street, 76-453, Cambridge, MA 02142, USA

Phone: 617-253-0893

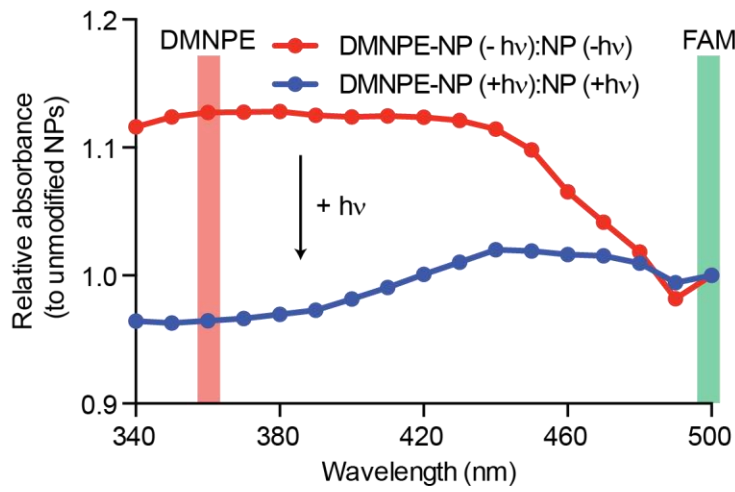
Fax: 617-324-0740

Email: sbhatia@mit.edu



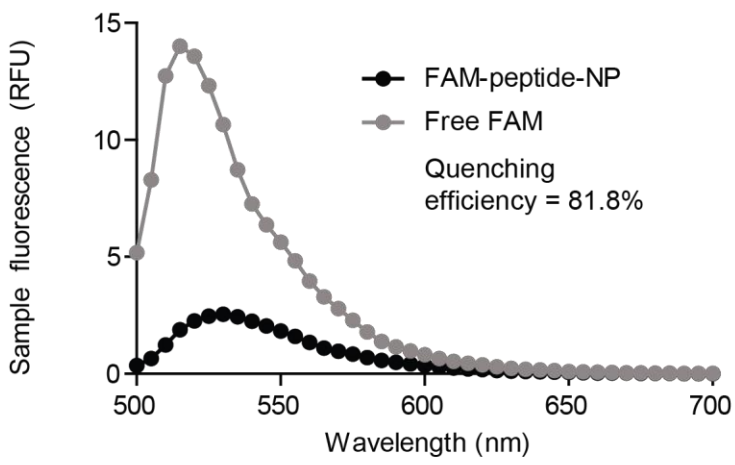
**Supplementary Figure 1. Design of protease sensing nanoparticles for *in vitro* applications.** (a) Dynamic light scattering measurement of nanoparticle size. (b) The *in vitro* protease sensor (C1-NPs) is comprised of a fluorescent reporter connected to the substrate and coupled to NPs.

a

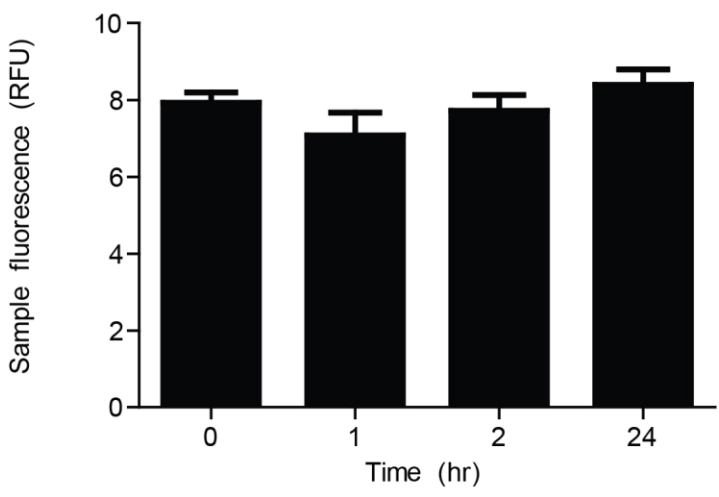


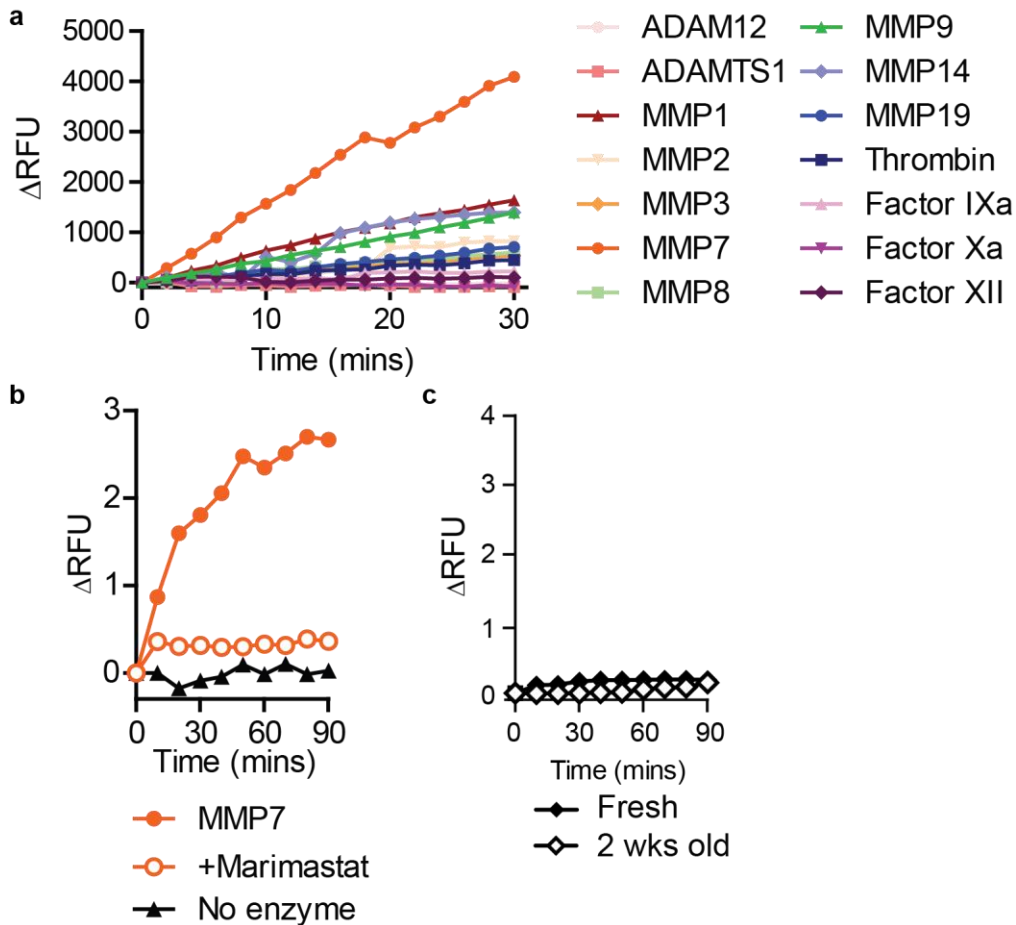
**Supplementary Figure 2. Nanoparticle and photolabile group characterization.** (a) Veiled sensors (DMNPE-NP) or unmodified sensors (NP) were exposed to light for 30 minutes, purified, and absorbance was compared to unexposed particles. The decrease in relative absorbance from the 300-400 nm window, indicates photolysis of the DMNPE. Normalized to the FAM absorbance ( $\lambda = 500$  nm). (b) Quenching on nanoparticles is achieved at high-valency coupling, in comparison to free FAM (Excitation: 470 nm; emission: 500-700 nm; cutoff: 495 nm; quenching efficiency = 81.8%). (c) Nanoparticles were added to human control serum and fluorescence was measured over 24 hours. No dequenching was observed.

b

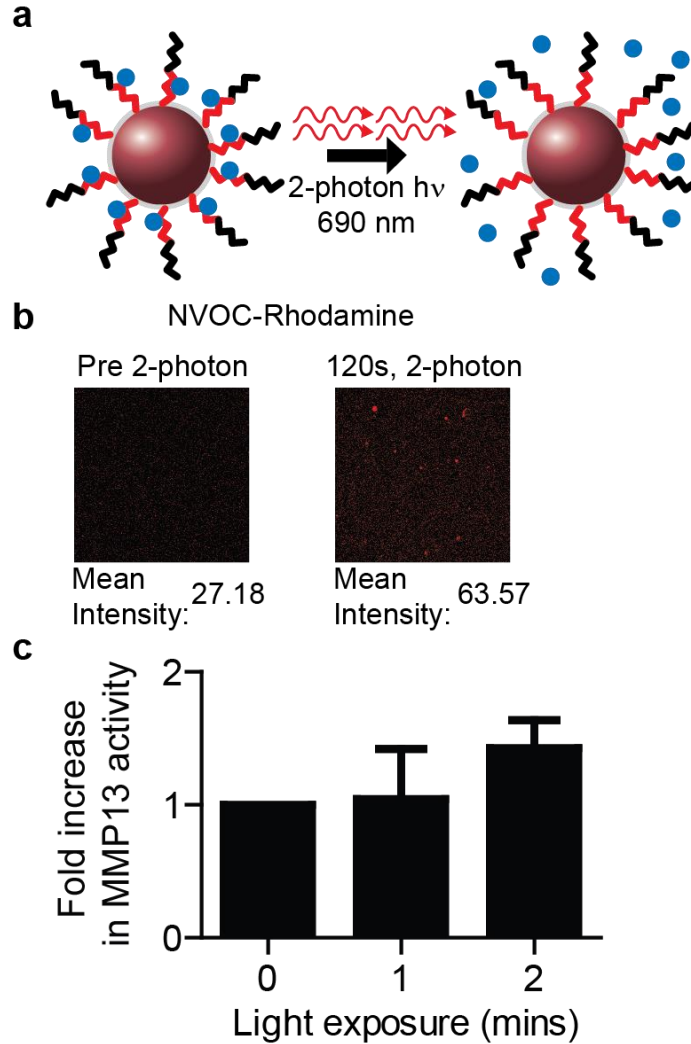


c

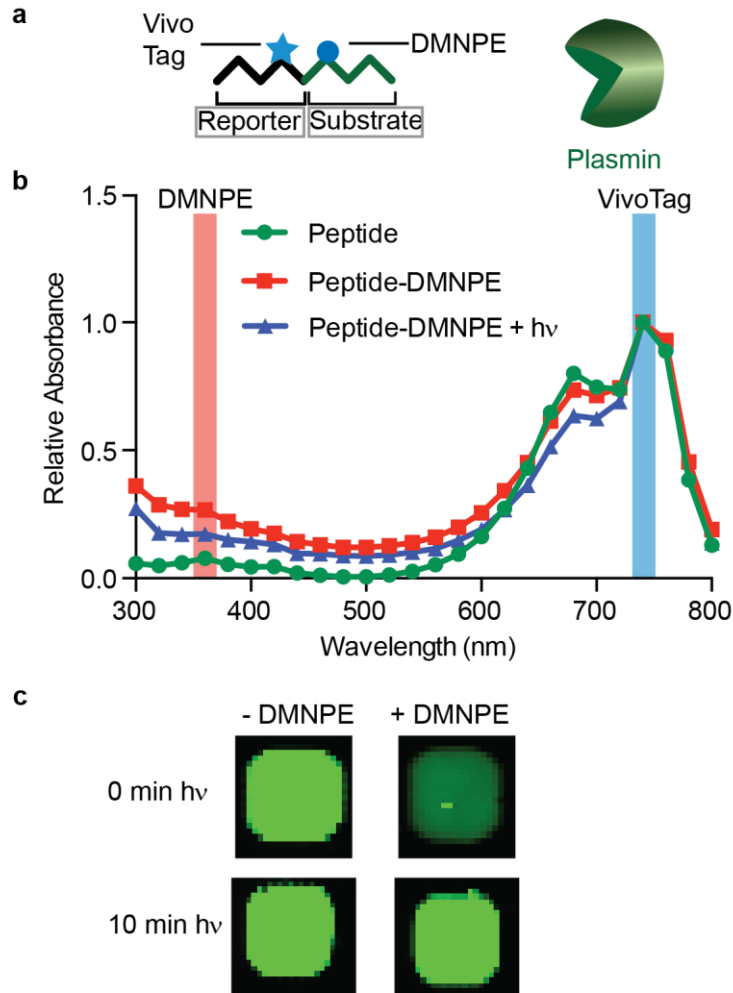




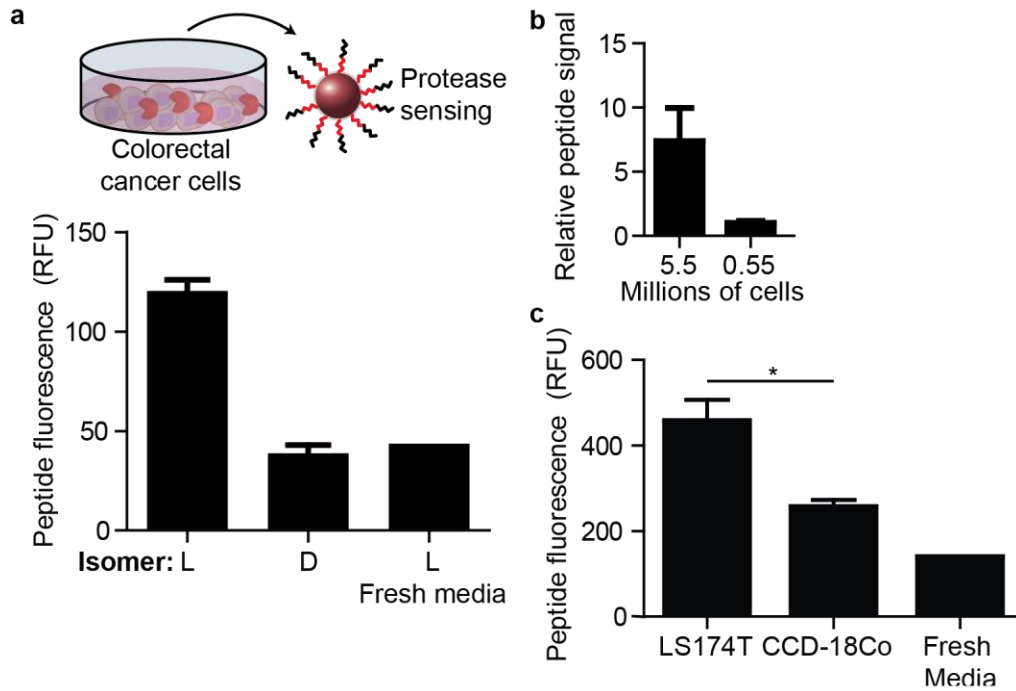
**Supplementary Figure 3. Biochemical characterization of substrate susceptibility of substrate to proteases.** (a) Subset of proteases from Fig. 3a that can cleave the substrate. (b) Marmimastat, an MMP inhibitor, abrogates cleavage showing fluorescence is generated through proteolysis. (c) DMNPE conjugation is stable. Samples tested for proteolysis against MMP9 two weeks after conjugation perform similarly to freshly coupled DMNPE-peptide conjugates.



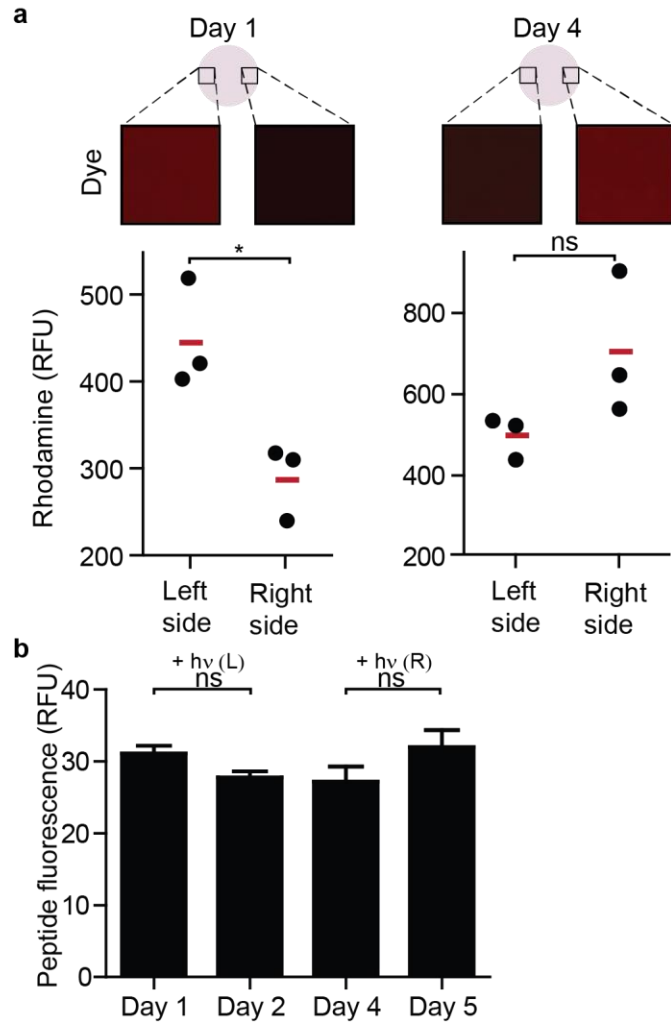
**Supplementary Figure 4. STREAMs can be unveiled by two-photon light.** (a) Two-photon light at 690 nm is able to unveil the STREAM particles. (b) NVOC-rhodamine was used to test if exposure to two-photon light for 120 seconds would cause an increase in rhodamine fluorescence. Mean rhodamine intensity increased after light exposure. (c) Two-photon unveiled STREAMs were exposed to MMP13 and activity was measured. MMP13 activity against the substrates increased with two-photon unveiling ( $n = 2$ ,  $\pm$  s.e.m.; 50% power of laser operating at 1 W).



**Supplementary Figure 5. Application of photolabile group to alternate substrate. (a)** Alternate substrate/reporter pair were veiled by DMNPE and tested against plasmin. **(b)** Addition of DMNPE is confirmed by shifts in absorbance from 300 – 400 nm. Photolysis shifts the absorbance back towards unmodified. **(c)** Proteolysis is mitigated by DMNPE veiling, which is recovered by light unveiling.

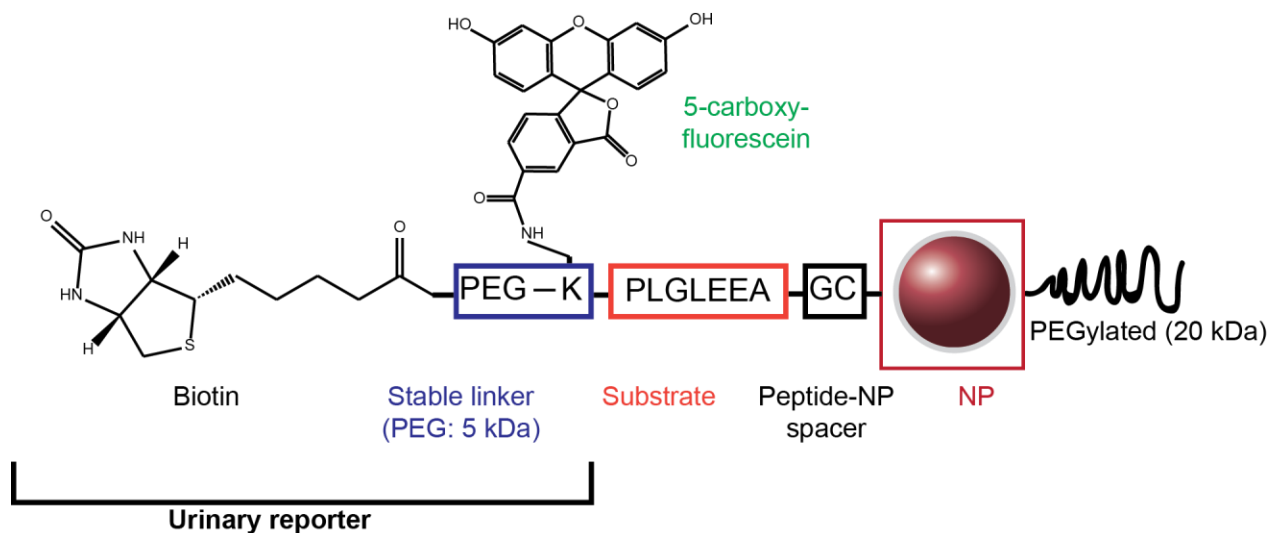


**Supplementary Figure 6. Cellular proteases can cleave protease sensors. (a)** C1-NPs were exposed to supernatant from colorectal cancer cells (LS174Ts) to determine if they can detect protease activity of a cellular origin. D-amino acid control sequence: c1, FAM-sk-pIGleea-GC. **(b)** Protease sensors are sensitive to cellular concentration by incubating sensors at the same concentration in conditioned media from high or low-density cell cultures. **(c)** Secreted proteases from normal fibroblast cells (CCD-18Co cell line) cleaved the sensor to a lesser extent (n = 3, s.e.m. for a-c, \* $P < 0.05$ , Student's *t*-test).

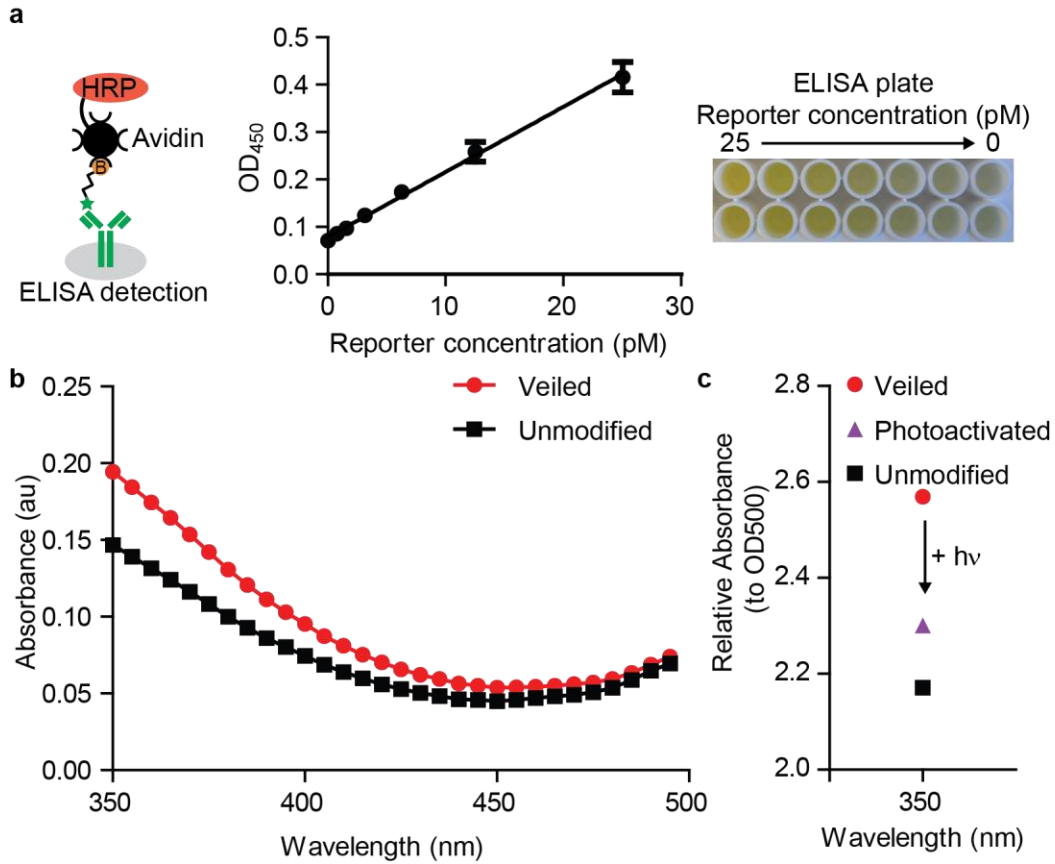


**Supplementary Figure 7. Characterization of collagen cancer model.** (a) Fluorescence of light-sensitive rhodamine. After light activation on the left half of the gel, rhodamine fluorescence is visualized on the left side. Quantification of rhodamine intensity on either side of the gel. Increases can be detected in the side corresponding with side that was illuminated ( $*P < 0.05$ ,  $ns P > 0.05$ , two-tail, Student's  $t$ -test). (b) Unmodified substrates were also embedded in another set of collagen cancer tissues. The signal for these stays high throughout (compared to protected; see figure 4b-c) and is unaffected by light exposure. Similar to protected sensors, the left half of gels was exposed on Day 1 and the right half on Day 4 ( $ns$ ,  $P > 0.05$ , two-tail, paired Student's  $t$ -test,  $n = 3$ , s.e.m.).

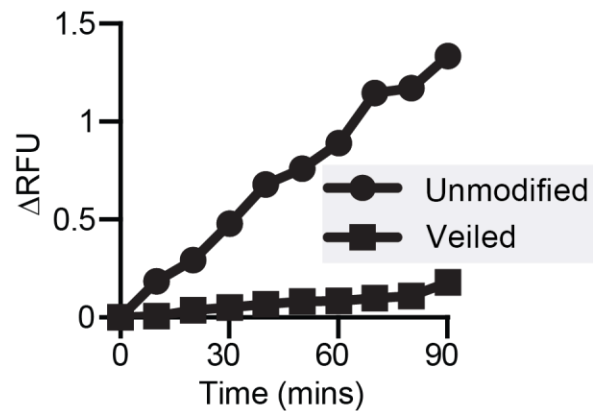




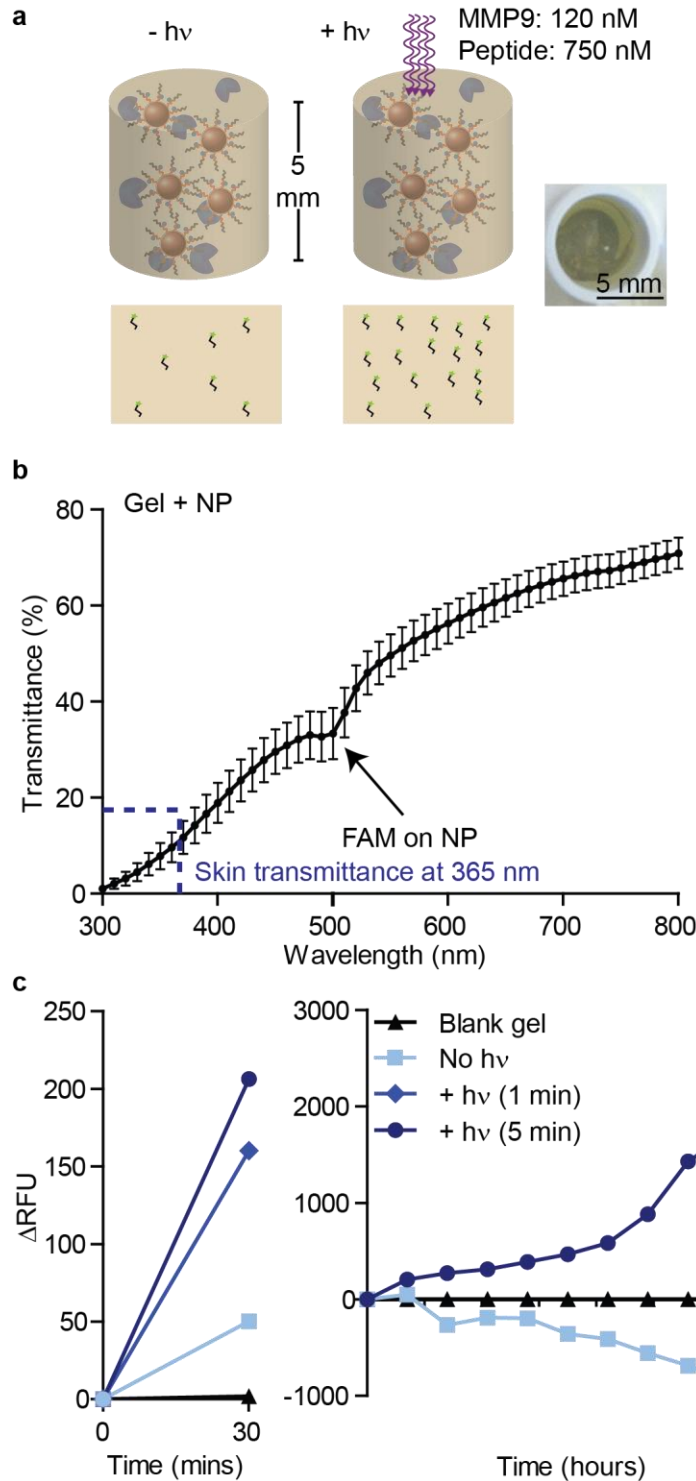
**Supplementary Figure 8. Design of *in vivo* STREAM synthetic biomarkers.** The *in vivo* protease sensor (V1-NPs) is comprised of a urinary reporter that clears through kidney into urine where it can be detected using a customized sandwich ELISA, coupled to the substrate.



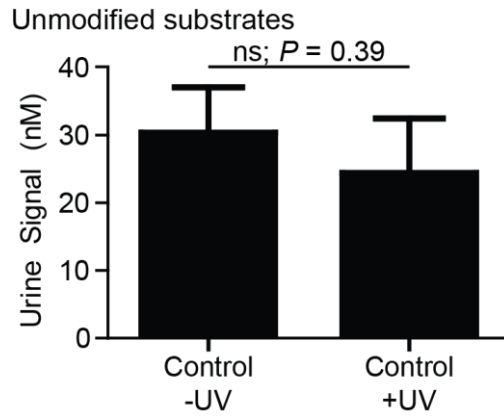
**Supplementary Figure 9. *In vivo* assay analysis.** (a) Sandwich ELISA characterization shows strong linear signal corresponding to reporter concentration. ELISA can detect low picomolar concentrations making it amenable for urine-based protease activity measurements ( $n = 2$ , s.d.). (b) Absorbance spectra of nanoparticles used in experiments described in **Figure 5a**. The same quantity of peptide for unmodified and veiled was injected in mice. (c) After light activation of protected peptides, relative absorbance at 350 nm associated with DMNPE decreases down closer to unprotected substrates.



**Supplementary Figure 10. STREAMs are protected from non-specific cleavage by thrombin.** Recombinant thrombin, a representative blood protease, elicits reduced proteolysis of the veiled sensors enabling a decrease in background blood signal. C1-NPs (unmodified or veiled) were exposed at the same concentration to thrombin and cleavage was monitored by fluorescence release.



**Supplementary Figure 11. 3D agarose hydrogel demonstration.** (a) Agarose hydrogels were embedded with STREAMs and recombinant MMP9 at concentrations approximately expected *in vivo*. (b) Agarose hydrogels have similar transmission to skin at 365 nm. This is important as it serves to validate that light activation through skin is feasible. (c) Light activation of 1 minute is sufficient to drastically increase the proteolysis measurements made in the hydrogel. Signal generated can be measured over several hours (200 mW/cm<sup>2</sup>).



**Supplementary Figure 12. UV exposure does not affect urinary signal.** Healthy nude mice were exposed to UV as before and then infused with unmodified synthetic biomarkers. Urine was collected 30 minutes later and compared to urine from mice that had not been exposed to UV. (n = 3, error bars:  $\pm$  SD, two tail Student's *t*-test).